Chem. Chem. Technol., 2023, Vol. 17, No. 4, pp. 903–915

Chemical Technology

FABRICATION OF ACTIVATED CARBON/CHITOSAN HYBRID MATERIAL FOR ADSORPTIVE REMOVAL OF Pb(II)

Rajith A. Perera[1], Ruwan T. Perera[2], Chandima. S. K. Rajapakse[1,✉]

https://doi.org/10.23939/chcht17.04.903

Abstract. In this study, a novel, cost-effective and environmentally friendly activated carbon/chitosan hybrid material (ACCHM) was synthesized by incorporating surface properties of both the activated carbon derived from rice husk and chitosan extracted from "Black Tiger" shrimp shells to generate a highly functionalized porous material with enhanced Pb(II) adsorption capacity for water purification.

Keywords: activated carbon, adsorptive removal, biomass, chitosan, lead, porous material.

1. Introduction

Heavy metal toxicity has proven to be a significant threat due to the numerous health risks associated with it. Hence in recent years, the importance of removing heavy metal ions from aqueous solutions for pollution control has grown.[1-4] Due to the rapid growth of industries including metal plating and coating, mining, fertilizer, tanneries, batteries, paper, and pesticides, heavy metal contaminated wastewaters are being released into the environment more frequently, either directly or indirectly.[5] Because of that, heavy metals have been found in large quantities in industrial waste streams. Hence, most of the novel studies have focused on the removal of heavy metal methodologies and techniques. Among them, heavy metal removal by the adsorption process is considered to be effective and required low investment for design and operation. Furthermore, as adsorption is reversible, adsorbents can be regenerated using suitable desorption processes.[6, 7]

Activated carbon (AC) is widely used in heavy metal mitigation from contaminated water. Its utility stems primarily from its high surface area as well as large micropore and mesopore volumes. Many research studies are conducted on the cost-effective removal of pollutants from aqueous solutions by AC.[8-11] However, the depletion of commercial coal-based activated carbon sources has resulted in price increases in recent years and therefore finding alternative sources for AC production from abundant and low-cost natural sources is a concern. It has been reported that carbonaceous materials can be converted into AC for heavy metal remediation[12-15] and as an example, AC derived from an eucalyptus bark could be used in the binary component sorption of Cu(II) and Pb(II), with maximum adsorption capacities of 0.45 and 0.53 mmol/g, respectively.[14] In addition to that, poultry litter-based activated carbon has significantly higher adsorption affinity and capacity than the commercial activated carbon.[15-17]

Meanwhile, due to the abundance, physical and chemical versatility, a wide range of value-added chitin and chitosan applications are being investigated and developed.[18] Chitosan is a biologically derived material. From a chemical viewpoint, chitosan is a poly D-glucosamine, a de-acetylated form of chitin (a natural polymer found in a variety of sources, including crustaceans and fungal cell walls) and it has numerous applications in biochemistry, pharmacy, medicine, agriculture, apart from the wastewater treatment.[19] Preparation of hybrid material by coating biologically origin material (chitosan) on the AC permits to modify and improve the surface properties of chitosan. Due to this modification, much less AC is required for the contaminant removal process. It has also been more cost-effective and environmentally friendly.[20] Also, owing to the combining of unique surface properties of both AC and chitosan, a wide range of metals and other impurities can be mitigated. Along with it, most studies proved that activated carbon/chitosan composites have excellent adsorption capabilities for water purification purposes. As an example, a recent study revealed that, chitosan/activated carbon composite had removed 100% of Cd(II) from the simulated water.[21] In addition to that, an adsorption study on Pb(II) using chitosan/TiO_2 hybrid film (CTF) was also reported and the theoretical Pb(II) adsorption efficiency of the CTF was 90.6% under optimum conditions (at pH 3-4, 333 K, and the initial metal concentration of 50–55 mg/L).[6]

[1] Department of Chemistry, Faculty of Science, University of Kelaniya, Sri Lanka
[2] Department of Indigenous Medical Resources, Faculty of Indigenous Health Sciences and Technology, Gampaha Wickramarachchi University of Indigenous Medicine, Sri Lanka
✉ *shashikala@kln.ac.lk*

In this study, our intention was to synthesize a hybrid material by coating chitosan on the activated carbon derived from rice husk to improve the surface activity of chitosan as a cost-effective and eco-friendly adsorbent for efficient mitigation of Pb(II) from aqueous solutions. The activated carbon/chitosan hybrid material (ACCHM) was developed as a novel material to embrace the surface properties of both materials for the purification process of contaminated water.

Experimental

2.1. Materials

Chemicals and standards of analytical grade were used as received from Sigma-Aldrich (USA), BDH (UK) or Fluke (Switzerland). The experiment was conducted using deionized water. Shrimp shells were collected from the local fish market and rice husks were collected from a rice mill at Piliyandala, Sri Lanka.

2.2. Extraction and characterization of chitosan

In order to extract chitin, first, powder of "Black Tiger" shrimp shell was immersed in HCl (7%, v/v) solution with the concentration of 100 g/L at room temperature for 24 h for demineralization purposes. The mixture was then filtered through a filter paper, and the residue was washed with distilled water. The residue was deproteinized by immersing it in NaOH (10% (w/v)) at room temperature for 24 hours and filtered to remove the proteins, and the residue was washed with distilled water until the washings became pH 7. The crude chitin was dehydrated sequentially with 95% and 100% ethanol before being dried at 323 K for 15 h. To make crude chitosan, the extracted chitin was placed in NaOH (50% (w/v)) at 383 K for 4 hours. The mixture was then filtered, and the residue was washed with hot distilled water at 333 K. This procedure was repeated three times. The raw chitosan was collected and dried 15 h at 323 K. Using Eq. (1), the degree of deacetylation or deacetylation percentage (DA%) of extracted chitosan was calculated.

$$\text{Degree of deacetylation} = 97.67 - \left(26.486 \left(\frac{A_{1655}}{A_{3450}}\right)\right) \quad (1)$$

where A_{1655} = absorbance of the amide I band at 1655 cm^{-1} and A_{3450} = absorbance of the hydroxyl band.[22]

Scanning Electron Microscopy & Energy Dispersive Spectroscopy (SEM/EDAX) and Fourier Transform Infrared Spectroscopy (FTIR) were used to characterize the chitosan.

FT-IR: FTIR spectrum of chitosan was obtained from an FTIR Spectrophotometer (ALPHA-T, Bruker, Germany). The chitosan sample was prepared as a potassium bromide (KBr) disk. 10-20 mg of chitosan powder and 1 g of KBr were mixed for 10 minutes with an agate mortar and pestle and a KBr pellet was prepared. The pellet was scanned in the range of 600-1400 cm^{-1} and the spectrum was obtained via Opus 6.5 version software package with 4 cm^{-1} resolutions, 16 scans as a sample scan time and 16 scans as background scan time.

SEM/EDAX: Scanning Electron Microscopy and Energy Dispersive Spectroscopy were used to investigate the surface morphology and elemental composition of the extracted chitosan. (ZEISS-EVO-18 REASERACH™).

2.3. Preparation of activated carbon (AC) derived from rice husk

Cleaned and dried rice husks samples (12.00 g) were carbonized at 673 K for 60-150 minutes (60 min (AC01), 90 min (AC02), 120 min (AC03), 150 min (AC04)) and chemically activated by HCl (5% v/v). The activated carbon yield in each sample was calculated using Eq. (2).

$$X\,(\%) = m/m_0 \times 100 \quad (2)$$

where X – yield of the activated carbon (%), m is the dry mass of the activated carbon (g) and m_0 is the raw sample mass (g).

2.4. Evaluation of the effect of carbonization time on Pb(II) removal % of activated carbon and characterization of activated carbon with the highest Pb(II) removal percentage

To determine the percentages of Pb(II) removed from AC prepared from rice husk at various carbonized temperatures, a Pb(II) standard solution (5.00 mg/L) was separately added to activated carbon samples (1.00 g, AC01, AC02, AC03, AC04) and stirred for 1 hour at pH 7 at room temperature. The solutions were then filtered, and the residual Pb(II) was determined using AAS (Atomic Absorption Spectroscopy) (Thermo scientific ICE 3300, GBC 932 plus). The activated carbon with the highest Pb(II) removal percentage was characterized by SEM/EDAX, FT-IR, and proximate analysis (moisture, ash, volatile matter, and fixed carbon content).

2.5. Moisture content

An activated carbon sample (1.00 g) was weighed to the nearest 0.5 mg in a pre-dried crucible with a lid. The container's lid was removed, and the container and lid were placed in a preheated oven (423 K). After 3 h, the crucible was closed immediately and cooled in a desiccator to an ambient temperature.

2.6. Volatile matter content

First, a crucible (preheated at 1223 ± 25 K for 30 min) was weighed to the nearest 0.1 mg. Activated carbon (5.00 g) was placed in the crucible and heated in a furnace at 1223 ± 25 K. After 10 minutes, the crucible was placed in the desiccator to cool to room temperature. Following that, the sample (crucible) was weighed and recorded.

2.7. Ash content

A crucible (preheated at 923 ± 25 K for 1 h) was weighed to the nearest 0.1 mg. Activated carbon (5.00 g) was placed in the crucible and heated at 923 ± 25 K in a furnace. After 16 h, the crucible was placed in a desiccator and allowed to cool to the ambient temperature. Then the sample (crucible) was weighed and recorded.

2.8. Bulk density

An activated carbon sample was placed in a graduated cylinder (200 mL). The cylinder was tapped continuously until flattened the top layer. The volume was read and recorded, and the procedure was repeated until the difference between the two observations was less than 2 mL. The content of the cylinder was weighed to the nearest 0.1 g. Bulk density was calculated using the Eq. (3).

$$\textit{Bulk density} = \textit{weight of dry material (g)} / \textit{volume of packed dry matter (mL)} \quad (3)$$

2.9. Preparation and characterization of activated carbon/chitosan hybrid material (ACCHM)

Activated carbon derived from rice husk (20.00 g) was placed in a beaker containing HCl (5% v/v) for 24 h to prepare acid-treated activated carbon. The activated carbon was then washed with deionized water and dried in a 343 K oven for 12 hours. Chitosan (3.00 g) was slowly added to 250 mL of acetic acid (1% v/v) solution under continuous stirring at 318-323 K to make chitosan gel. Acid-treated activated carbon (20.00 g) was added slowly to the chitosan gel and stirred for 16 h at 318–323 K. The activated carbon/chitosan hybrid material (ACCHM) was filtered from the solution and washed several times with deionized water until the washings reached a neutral pH. Then ACCHM was dried in an oven (323 K). Further, the ACCHM was characterized by SEM/EDAX (ZEISS EVO 18, Japan), and FT-IR (iS50 Thermo Scientific, USA).

2.10. Batch adsorption studies

2.10.1. Effect of initial metal ion concentration on the Pb(II) adsorption on ACCHM

The prepared ACCHM (approximate diameter 5.023 µm, 0.05 g) per container were taken separately to 7 clean dry polypropylene containers. Pb(II) solution (1 mg/L, 2 mg/L, 3 mg/L, 4 mg/L, 5 mg/L, 6 mg/L, 7 mg/L) was introduced separately into each polypropylene container having ACCHM (pH = 7). These samples were shaken at room temperature (303 ± 2 K) for 60 min. The samples (filtrates) were subjected to the AAS (Thermo scientific ICE 3300, GBC 932 plus) analysis to determine the residual Pb(II) concentrations. Data were used to calculate the Pb(II) adsorption capacities of ACCHM at each metal ion concentration used. Pb(II) adsorption capacity values were calculated using the Eq. (4).

$$\boldsymbol{Pb(II)\ adsorption\ capacity\ (q)} = \frac{adsorbed\ weight\ of\ Pb(II)\ on\ ACCHM(mg)}{weight\ of\ ACCHM\ used\ (g)} \quad (4)$$

2.10.2. Effect of initial ACCHM dosage on the Pb(II) adsorption on ACCHM

The prepared ACCHM samples (0.01 g, 0.02 g, 0.04 g, 0.05 g, 0.06 g, 0.07 g, 0.08 g) were taken separately to clean dry polypropylene containers. A volume of Pb(II) solution (50.00 mL, pH=7, 2 mg/L) was introduced into each polypropylene container having ACCHM. These samples were shaken at room temperature (303 ± 2 K) for 60 min. Control samples were prepared using above mentioned doses and deionized water (50.00 mL) and a similar experiment was carried out simultaneously. The residual Pb(II) of the filtrates was determined using AAS. The data was used to calculate the percent removal of Pb(II) by ACCHM at various ACCHM dosages.

$$\%\boldsymbol{Pb\ (II)removal} = \frac{weight\ of\ Pb\ (II)removed\ (mg)}{weight\ of\ initial\ Pb\ (II)(mg)}\ x\ 100 \quad (5)$$

2.10.3. Effect of shaking time on the adsorption of Pb(II) on ACCHM

The prepared ACCHM samples (0.05 g) per container were taken separately to 7 clean dry polypropylene containers. A volume of Pb(II) solution (50.00 mL, pH=7, 2 mg/L) was introduced into each polypropylene container having ACCHM. At room temperature (303 ± 2 K) these samples were shaken separately (20 min, 30 min, 60 min, 90 min, 120 min, 150 min, 180 min). Control samples were prepared using above mentioned doses and deionized water (50.00 mL) and a similar experiment was carried out simultaneously. Then the samples were subjected to AAS analysis. The data were used to measure

the percent removal of Pb(II) by ACCHM at various shaking times.

2.10.4. Effect of pH on the Pb(II) adsorption on ACCHM

The prepared ACCHM samples (0.05 g) per container were taken separately to 6 clean dry polypropylene containers. pH was adjusted (2 pH, 3 pH, 5 pH, 7 pH, 9 pH, 11 pH) and Pb(II) solution (2 mg/L, 50.00 mL) was introduced separately into each polypropylene container having ACCHM. These samples were shaken at room temperature (303 ± 2 K) for 120 min and filtered. Control samples were prepared using above mentioned pH and deionized water (50.00 mL) and similar experiments were conducted simultaneously. Then the samples were subjected to AAS analysis. The data were used to calculate the percent removal of Pb(II) by ACCHM at various pH levels.

2.10.5. Modeling of adsorption isotherm

The prepared ACCHM samples (0.05 g) per container were taken separately to 10 clean dry polypropylene containers. Pb(II) solution (1 mg/L, 2 mg/L, 3 mg/L, 4 mg/L, 5 mg/L, 6 mg/L, 7 mg/L, 8 mg/L, 9 mg/L, 10 mg/L, pH 7) was introduced separately into each polypropylene container having ACCHM. These samples were shaken at room temperature (303 ± 2 K) for 120 min. Control samples were prepared using above mentioned doses and deionized water (50.00 mL) and a similar experiment was carried out simultaneously. After shaking, all the samples were filtered. Then the samples and controls were analyzed by an Inductive Coupled Plasma-Mass Spectrophotometer (ICP-MS, Agilent 7800).

2.11. Kinetic studies

A Pb(II) solution (2 mg/L) was added to a clean dry polypropylene container containing ACCHM (0.05 g). The value of solution pH was adjusted to 5. The solution was continuously agitated in a shaker at 60 rpm at room temperature (303 ± 2 K). 10 mL aliquots were drawn at predefined time intervals for 180 minutes, filtered through a 0.45 µm nylon filter membrane, and the filtrates were analyzed for residual Pb(II) ion using ICP-MS. The Pb(II) adsorption capacity of ACCHM in each sample was calculated using Eq. (4).

2.12. Statistical analysis

All experiments were carried out in a duplicate, and results were reported as mean ± standard deviation.

3. Results and Discussion

3.1. Preparation of Chitosan

The deacetylation percentage (DA%) of prepared chitosan was found to be 82%. The DA% is an important parameter affecting solubility, chemical reactivity, metal adsorption capacity and biodegradability of chitosan. The DA% is calculated to determine how far the acetyl groups have been removed. Deacetylation improves the adsorption properties of chitosan by providing more sites for metal ion adsorption.

3.2. Preparation of activated carbon derived from rice husk

Here, HCl was used as an activating agent instead of the commonly used H_3PO_4. First, optimization of carbonaceous time was carried out by conducting the experiment at different carbonization times (60 min, 90 min, 120 min, 150 min) at 673 K and Pb(II) removal potentials of AC prepared at different carbonization times were evaluated under the selected experimental conditions. The results revealed that the yield % of AC was dependent on the carbonization time and the highest yield % of AC was reported at the 120 minutes of carbonaceous time (Fig. 1). Pb(II) removal % from activated carbon was varied between 55.07 % and 93.30 % at different carbonization times. The highest Pb(II) removal % was observed when the material was carbonized at 120 min, as depicted in Fig. 2. However, when the carbonization time was increased above 120 min, Pb(II) adsorption potential of AC was reduced (Fig. 2). This may be due to the fact that the pores were sintered due to a prolonged exposure to higher temperatures.[23] Therefore, it can be concluded that the metal adsorption capacity of AC is affected by the carbonization time.

3.3. Proximate analysis of activated carbon derived from rice husk

The proximate analysis gives the composition of a material in terms of gross components such as moisture, volatile matter, ash, and fixed carbon contents. The proximate composition of activated carbon was found to be 34.94 wt.% moisture, 32.47 wt.% ash, 24.20 wt.% volatile matter, and 8.39 wt.% fixed carbon, which makes it a suitable adsorbent. Meanwhile, the bulk density of the synthesized AC is 322.25 $kg \cdot m^{-3}$. If the bulk density is lower, AC's porosity will increase, thus expanding the surface area for adsorption.[23]

3.4. Preparation of activated carbon/chitosan hybrid material (ACCHM)

In this study, ACCHM (Fig. 3, b) was prepared by coating chitosan on activated carbon derived from rice husk (Fig. 3a) carbonized at 120 min at 673 K temperature. Chitosan loading in AC support was about 25% by weight. Here, chitosan was physically modified in order to improve the mechanical strength, chemical stability and metal adsorption capacity of the adsorbent.

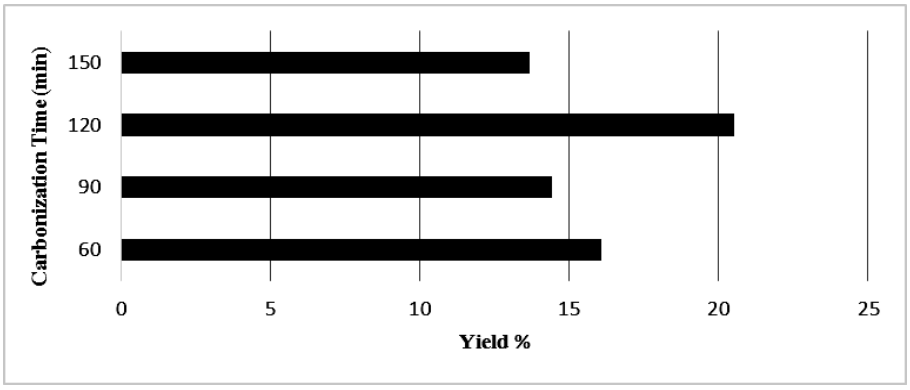

Fig. 1. Effect of carbonization time (min) on yield % of AC

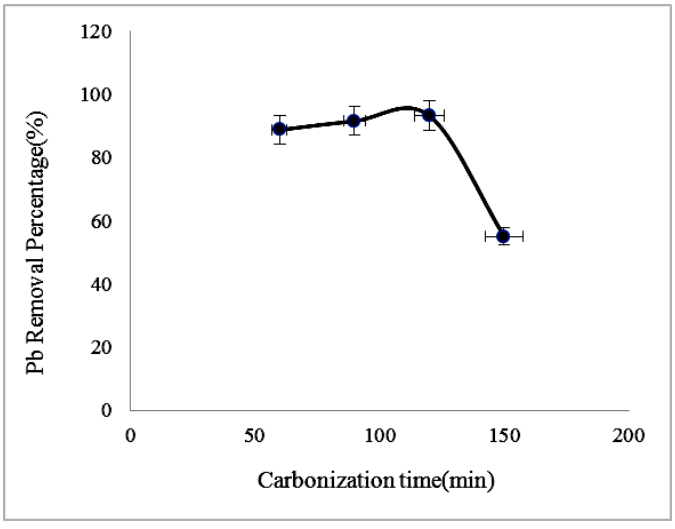

Fig. 2. Effect of carbonization time on Pb(II) removal percentage

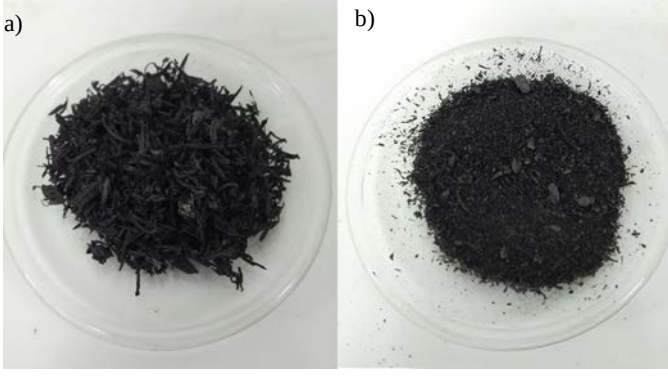

Fig. 3. (a) Activated carbon (AC) derived from rice husk and (b) ACCHM

3.5. Spectral characterization of synthesized materials

IR spectra of chitosan, AC derived from rice husk, ACCHM and Pb adsorbed ACCHM are shown in Fig 4. The prominent bands of the IR spectrum of chitosan (Fig. 4a) include a strong broad band at the wavenumber region of 3400-3750 cm^{-1}, corresponding to O–H stretching vibrations and multiple stretching vibrations of $–NH_2$.[24,25] The bands appear at 2870 cm^{-1} and 2930 cm^{-1} correspond to C–H stretching of $–CH_3$ and $–CH_2$, respectively. Further, a band appeared at 1580 cm^{-1} for primary amine's N–H bending vibration[25] confirming the successful extraction of chitosan from shrimp shells by deacetylation of chitin. The major bands of the IR spectrum of AC (Fig. 4b) include bands at 3220-3364 cm^{-1} (stretching vibration of –O–H), 1598 cm^{-1} (strong) (stretching vibration of –C=O), and 1062 cm^{-1} (stretching vibration of Si–O).

When consider the IR spectrum of the novel hybrid material, ACCHM (Fig. 4c), an absorption band at 1598 cm^{-1} can be attributed to the C=O stretching of N-acetyl groups, and a band at 1366 cm^{-1} can be attributed to the –NH deformation vibration in $–NH_2$ of chitosan of the hybrid material. The peaks at the wave number region of 1548–1602 cm^{-1} in the FTIR spectrum of ACCHM correspond to N–H bending vibrations, including N–H scissoring of the amines. Peaks at 2970 cm^{-1}, 2855 cm^{-1}, 1228 cm^{-1}, and 1216 cm^{-1} correspond to C–H aliphatic stretching, stretching vibration of $–O–CH_3$, stretching vibrations of C–O in carbonyl, lactonic, and carboxyl groups, and stretching of C–O or O–H deformation in carboxylic acids in the hybrid material, respectively.[24,26] In addition to that, a broad peak appeared at 3000 cm^{-1}–3400 cm^{-1}, corresponding to O–H stretching vibrations and multiple stretching vibrations of $–NH_2$ as in the spectrum of chitosan (Fig. 4a). Hence, these findings confirmed that chitosan was successfully coated on AC producing an activated carbon/chitosan hybrid material.

When comparing the FTIR spectra of the ACCHM and Pb absorbed ACCHM, major peaks have shifted after adsorption of Pb owing to the contribution of the surface functional groups of the ACCHM for metal ion adsorption. (Fig. 4d). It has already been known that upon binding of adsorbate with adsorbent, the IR bands in the close vicinity of the binding site of adsorbent are shifted when compared with the major peaks of adsorbate-free adsorbent.[1]

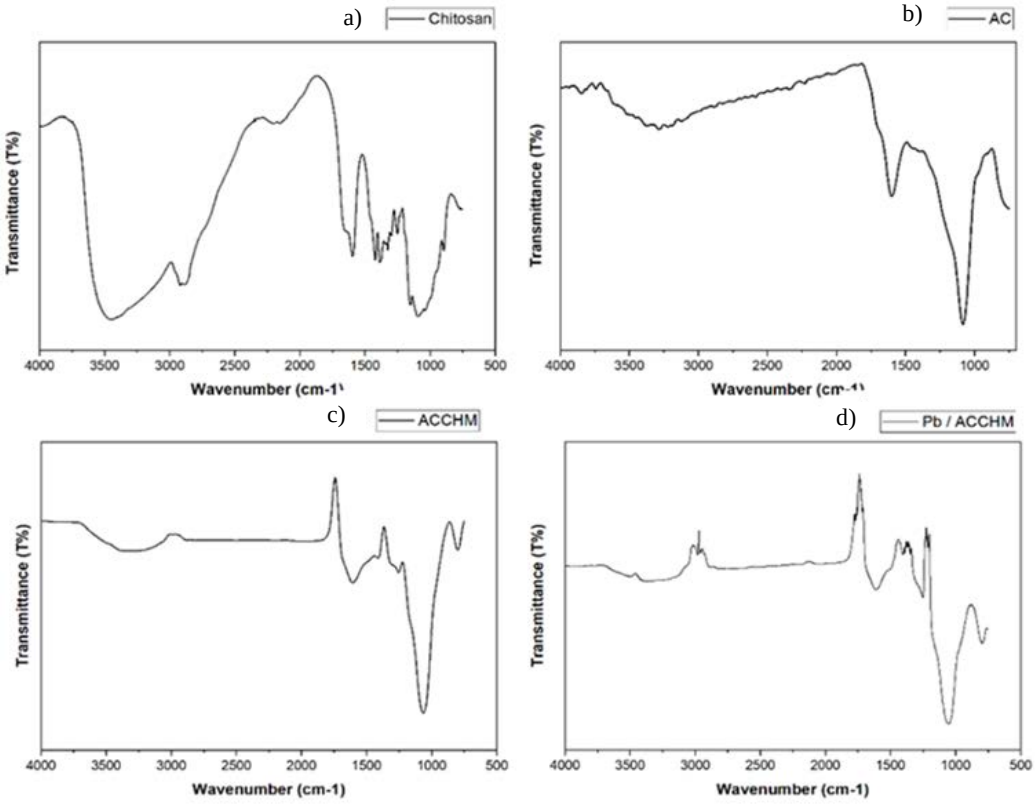

Fig. 4. FTIR spectra of (a) chitosan, (b) activated carbon (AC) (c) chitosan coated activated carbon (ACCHM), and (d) Pb adsorbed ACCHM

3.6. Characterization of synthesized materials by Scanning Electron Microscopy and Energy Dispersive X-ray Analysis

The surface morphology of the extracted chitosan shown in Fig. 5a depicts that chitosan has a smooth surface without a porous structure. Meanwhile, as depicted in Fig. 5b, c, the AC synthesized from rice husks has an irregular surface and a well-developed porous structure. The average pore diameter of AC calculated using ImageJ software was found to be 6 µm and upon coating of chitosan to prepare ACCHM the pore diameter has changed to about 7 µm.

In this study, a novel ACCHM was developed by coating chitosan on AC to blend the surface properties of chitosan and AC in order to improve the Pb(II) adsorption capacity.

Fig. 6 shows the surface morphology of ACCHM. Here, chitosan formed a rigid highly porous matrix layer on the surface of AC, which could enhance the adsorption of metal ions as activated carbon provides solid support to make all the binding sites accessible in addition to enhancing the surface area. The highly porous surface structure of the ACCHM (Fig. 6b) having functional groups of chitosan may act as a multi-functional absorbent as both physisorption and chemisorption of sorbate can take place.

EDAX was used to analyze the elemental composition of the solid surfaces of chitosan, AC, ACCHM, and ACCHM after adsorption of Pb (Fig. 7) and the results are tabulated in Table 1. The main elements present in AC are C (47.69%), O (37.07%), and Si (14.99%). The elemental composition of ACCHM is found to be C (68.73 wt.%), O (27.29%), Si (1.42%) and N (2.56 %). A peak for Pb was observed in the EDAX spectrum of Pb adsorbed ACCHM by confirming the adsorption of Pb(II) onto ACCHM under the selected experimental conditions.

Table 1. The elemental composition of chitosan, AC, ACCHM, ACCHM after adsorption of Pb

Material	Weight Composition (%wt)					
	C	O	Si	N	Cl	Pb
Chitosan	41.01	51.17		7.82		
AC	47.69	37.07	14.99		0.25	
ACCHM	68.73	27.29	1.42	2.56		
Pb /ACCHM	53.22	30.31	12.03	4.32		0.12

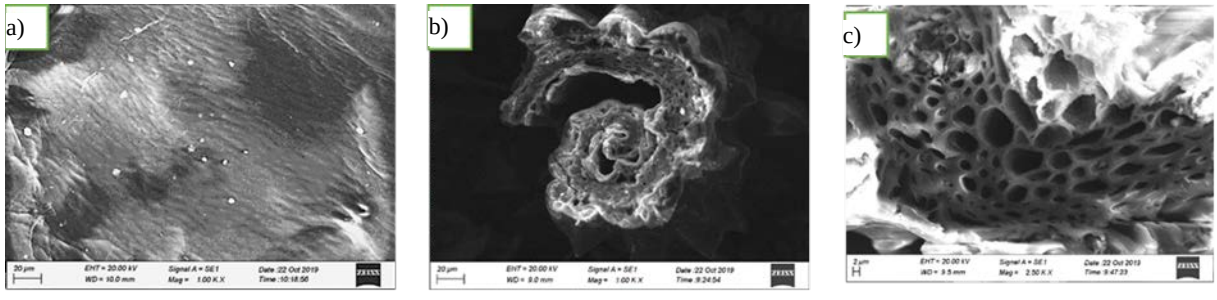

Fig. 5. SEM images of (a). Extracted chitosan - 1.00KX, (b). AC derived from rice husks – 1.00 KX, (c). AC derived from rice husks – 2.50 KX

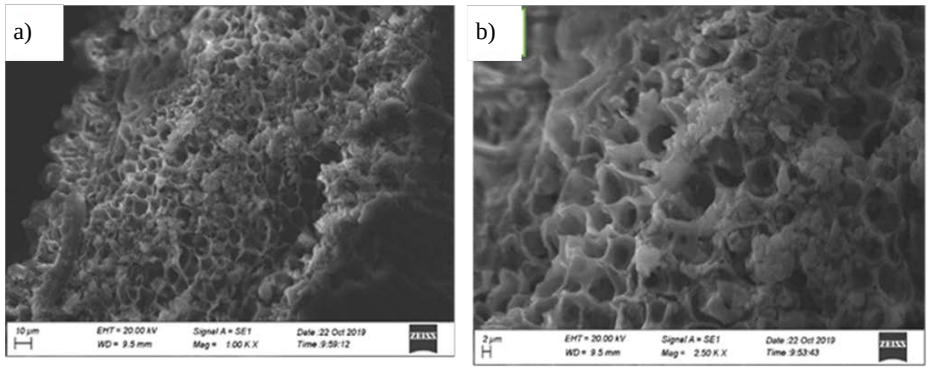

Fig. 6. SEM images of ACCHM under two magnifications, (a). 1.00 KX, (b). 2.50 KX

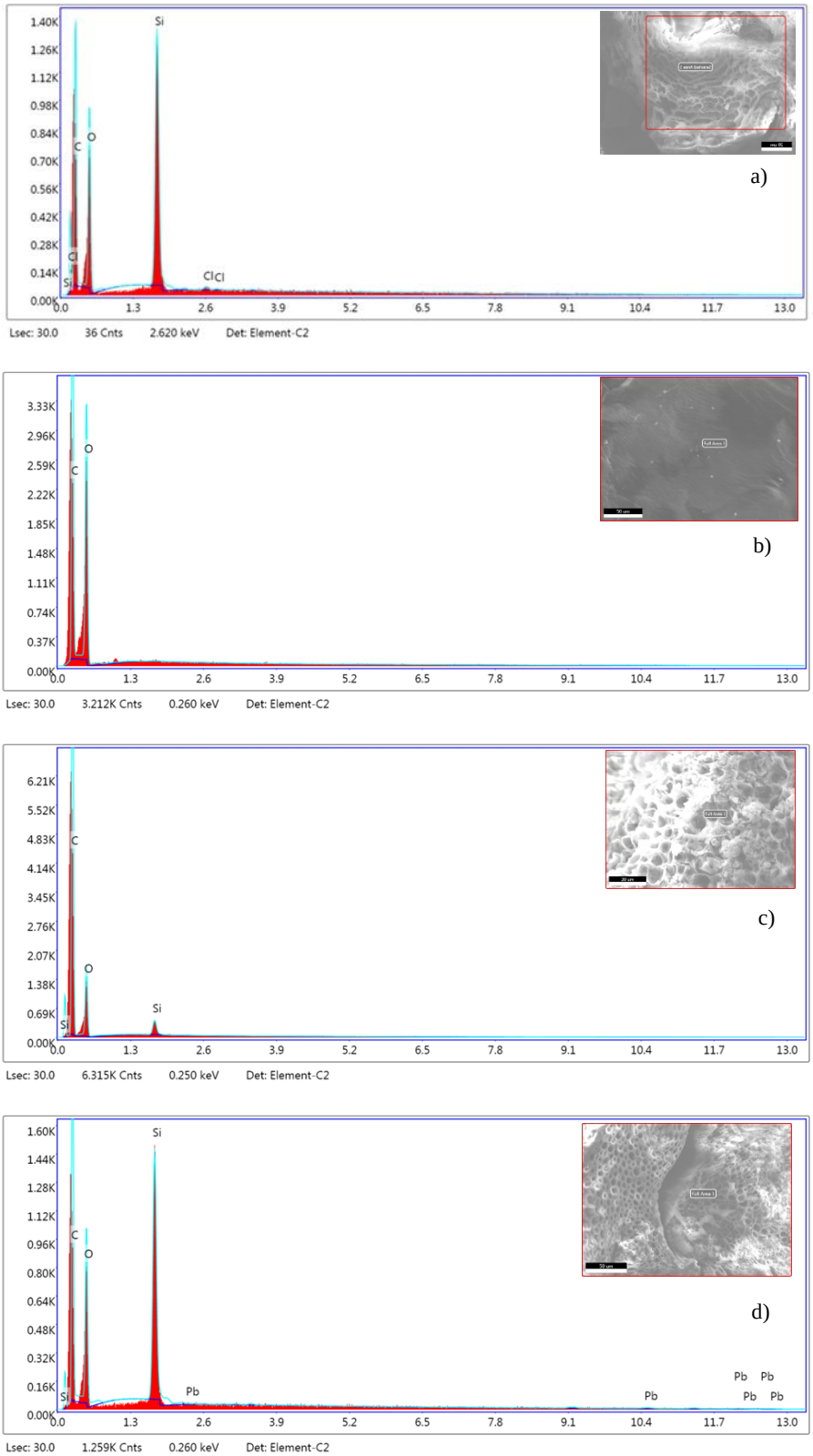

Fig. 7. EDAX spectra of (a). AC, (b). Chitosan, (c). ACCHM, (d). Pb adsorbed ACCHM

3.7. Batch adsorption studies for the optimization of process parameters

Batch experiments were conducted using synthetic wastewater solutions containing Pb(II) to determine the effect of initial Pb(II) ion concentration, ACCHM dosage, shaking time, and pH on Pb(II) adsorption capacity or percent of Pb(II) removal of the novel material, ACCHM. First, Pb(II) adsorption capacity (q) was calculated by varying the initial Pb(II) ion concentration (Fig. 8a). According to the graph, when the concentration increases, the q value keeps increasing. But the difference between q values decreased indicating that the adsorbent sites are gradually saturated as the Pb(II) concentration increased. A range of 0.01– 0.08 g of adsorbent dosage was used to study the effect of adsorbent dosage on percentage removal of Pb, and the experiments were carried out at a fixed Pb(II) concentration of 2 mg/L at pH 7 for a shaking time of 60 min (Fig. 8b). According to the results, the percentage removal of Pb(II) by ACCHM increased irregularly with the increasing adsorbent dosage to a maximum value (72%) and then upon further increasing, the percent of Pb(II) removal becomes constant as most of the adsorbate molecules adsorbed on the accessible binding sites of the adsorbent. Fig. 8c depicts the effect of shaking time on the percentage of Pb(II) removal. At the beginning, the percent removal of Pb(II) ion by ACCHM was increased rapidly due to the high availability of binding sites on the adsorbent. Then it becomes constant after 120 min indicating that the adsorbent gets saturated, and the system reaches the equilibrium.

Since solution pH plays a significant role for the metal ion adsorption process, optimization studies were conducted varying the solution's initial pH. According to the results, the maximum Pb removal percentage was obtained when pH of the solution was between pH 5 and pH 6 (Fig. 8d). When reducing pH of the solution, the surface of the adsorbent becomes positively charged, as a result, lower Pb(II) uptake was observed, which may be attributed to the corresponding electrostatic repulsions between Pb(II) and positively charged adsorbent sites. In addition, Pb(II) adsorption may further decrease due to the presence of excess H^+ ions, as they are competing with metal ions for the available sites.[21] From the batch studies it can be concluded that the maximum Pb removal percentage (89%) was observed at a solution with pH of 5, an initial Pb(II) concentration of 2 mg/L, an adsorbent dosage of 1 g/L, and a stirring time of 120 minutes.

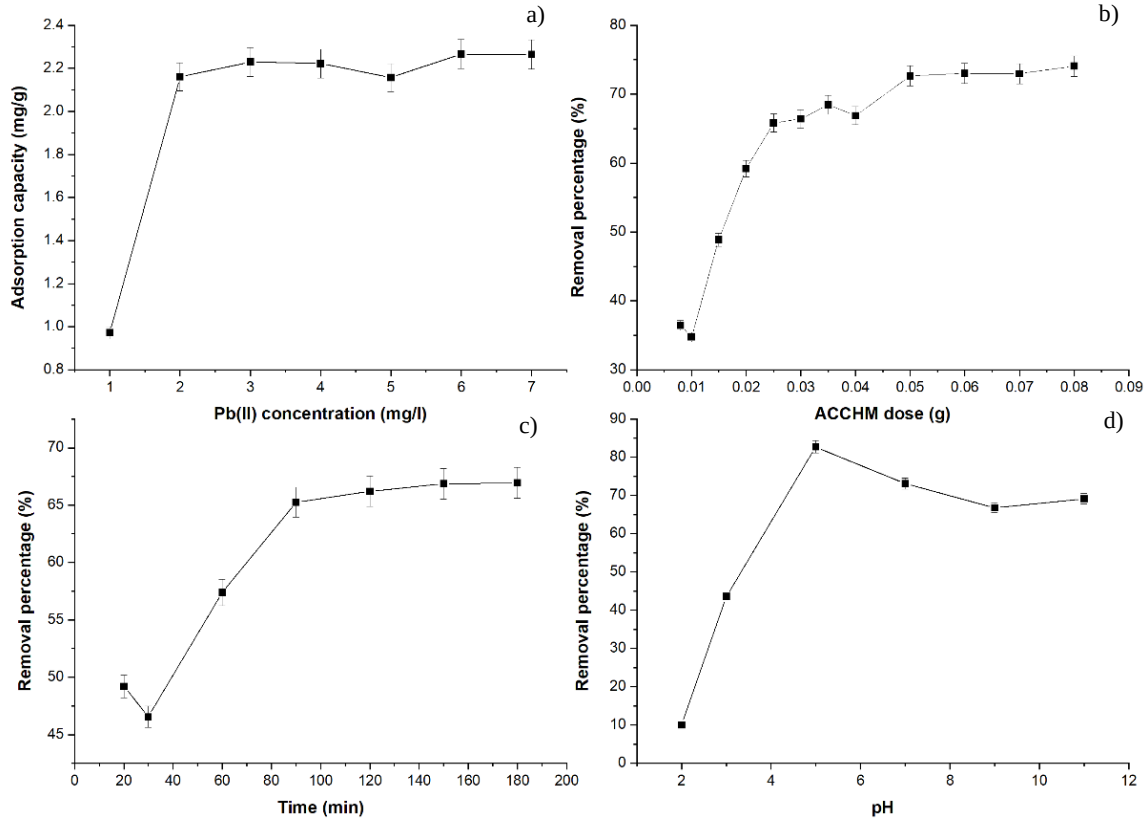

Fig. 8. Optimization studies of the batch process parameters of (a). initial Pb(II) concentration, (b). dosage of the adsorbent, ACCHM, (c) shaking time and (d). pH of the solution

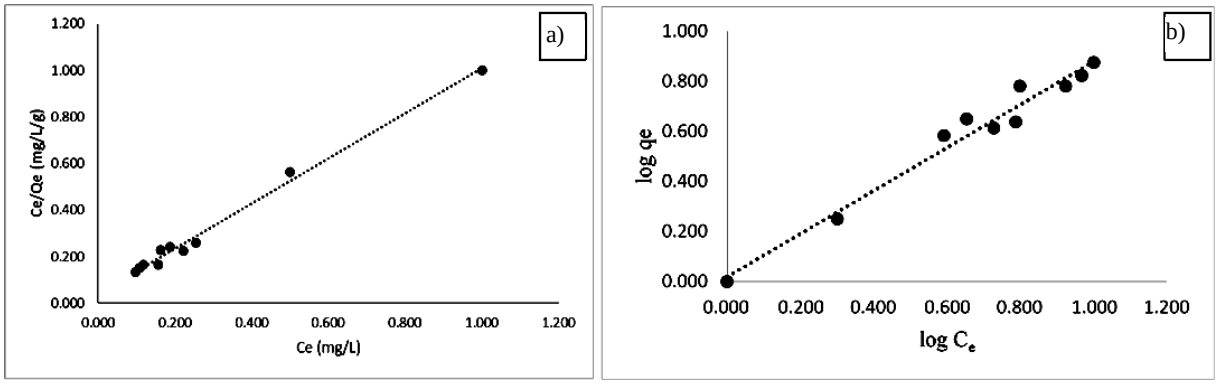

Fig. 9. (a). Langmuir adsorption isotherm of Pb sorption on ACCHM, (b). Freundlich adsorption isotherm of Pb sorption on ACCHM (adsorbent dose = 1 g/L, pH = 7±0.2, contact time = 120 minutes, initial concentration = 2 mg L^{-1}, agitation speed = 60 rpm, T=303 ± 2 K)

3.8. Modelling of adsorption isotherms of Pb adsorption on ACCHM

Adsorption isotherm models are commonly used to investigate the relationship between adsorption capacity (q_e) and aqueous adsorbate concentration (C_e) at equilibrium. Langmuir and Freundlich models were used in this study.

The Langmuir model assumes that the uptake of adsorbates occurs on a homogenous surface by a monolayer adsorption without any interaction between adsorbed ions.

The linearized form of the Langmuir equation is as follows[25,26]

$$\frac{C_e}{q_e} = \frac{1}{K_L \cdot Q_{max}} + \frac{C_e}{Q_{max}} \quad (6)$$

where, q_e is the equilibrium adsorption capacity (mg/g), Q_{max} is the maximum adsorption capacity (mg/g), C_e is the equilibrium aqueous concentration of adsorbate (mg/L), K_L is the constant related to the energy of adsorption (L/mg). A plot of C_e/q_e *vs.* C_e gives $1/Q_{max}$ as the slope and $1/K_LQ_{max}$ as the intercept.

Freundlich isotherm is based on a multilayer adsorption process on a heterogeneous surface. The model's linear form can be written as:[27]

$$log q_e = log K_F + \frac{1}{n} log C_e \quad (7)$$

where K_F and n are Freundlich constants that represent adsorption capacity and intensity, respectively; C_e is the equilibrium concentration in solution, q_e is the equilibrium adsorption capacity.

Experimentally obtained linear forms of the Langmuir and Freundlich isotherms are depicted in Fig. 9a and Fig. 9b respectively.

Table 2 lists the calculated Langmuir and Freundlich isotherm constants based on the experimental results. To determine the most relevant adsorption isotherm for the Pb adsorption on ACCHM, the correlation coefficient value (R^2) was considered. R^2 values for Langmuir and Freundlich adsorption isotherms were 0.9916 and 0.9700, respectively.

Table 2. Isotherm parameters for adsorption of Pb onto ACCHM

Langmuir Constants				Freundlich Constants		
Q_{max}(mg/g)	K_L (L/mg)	R_L	R^2	K_F	n	R^2
24.390	0.0423	0.9219	0.9916	1.04	1.16	0.9700

Since the adsorption data fit the Langmuir adsorption isotherm better than the Freundlich adsorption isotherm, it is concluded that the Langmuir model is an appropriate model to represent the adsorption equilibrium data of Pb(II) adsorption on ACCHM. It means that all active sites of the novel adsorbent, chitosan/AC hybrid material are homogeneous, and Pb metal ion uptake occurs *via* chemisorption as monolayer adsorption with no interaction between adsorbate molecules.

Langmuir constant, K_L can be used to calculate the equilibrium parameter (R_L), which is given by the following equation.

$$R_L = \frac{1}{1+K_L \cdot C_i} \quad (8)$$

where K_L is the Langmuir constant, C_i is the initial concentration.

The value of R_L indicates the type of Langmuir isotherm, whether it is irreversible ($R_L = 0$), linear ($R_L = 1$), unfavorable ($R_L > 1$), or favorable ($0 < R_L < 1$).[28]

Accordingly, the R_L value in this study was 0.9219, which indicates that Pb ion adsorption on the ACCHM surface is favorable. The maximum amount of adsorbate adsorbed per unit weight of adsorbent (Q_{max} value) was obtained corresponding to complete coverage of available sites from the Langmuir isotherm for ACCHM. Interestingly, our novel adsorbent, chitosan/AC hybrid material

has a higher Q_{max} value for Pb(II) adsorption (24.39 mg/g) compared to that of chitosan (10 mg/g) reported in the literature,[21] indicating that the physically modified hybrid bio adsorbent ACCHM has a higher adsorption capacity.

3.9. Adsorption kinetics

To understand the adsorption mechanism of Pb(II) on ACCHM, pseudo-first-order and pseudo-second-order kinetic models were used to analyze the experimentally obtained data. Lagergren's pseudo first-order kinetic model can be written as Eq. (9):[29]

$$ln(q_e - q_t) = lnq_e - (K_1\, t) \qquad (9)$$

where q_t and q_e are the amount of Pb ions adsorbed per mass of sorbent (mg/g) at any time and at equilibrium, respectively. K_1 is the first-order adsorption rate constant (min^{-1}).

The pseudo-second-order equation can be given as Eq. (10),[30]

$$\frac{t}{q_t} = \frac{1}{K_{2,ads}q_e^2} + \frac{t}{q_e} \qquad (10)$$

where q_t and q_e are the amount of Pb ions adsorbed per mass of sorbent (mg/g) at any time and at equilibrium, respectively. $K_{2.ads}$ is the rate constant of second-order adsorption (g (mg min) $^{-1}$).

The correlation coefficient of the pseudo-first order kinetic model is 0.8933 (Fig. 10a), while the correlation coefficient of the pseudo-second order kinetic model is 0.9955 (Fig. 10b). This indicates that a pseudo-second order kinetic model adequately described the adsorption kinetics of Pb adsorption on ACCHM.

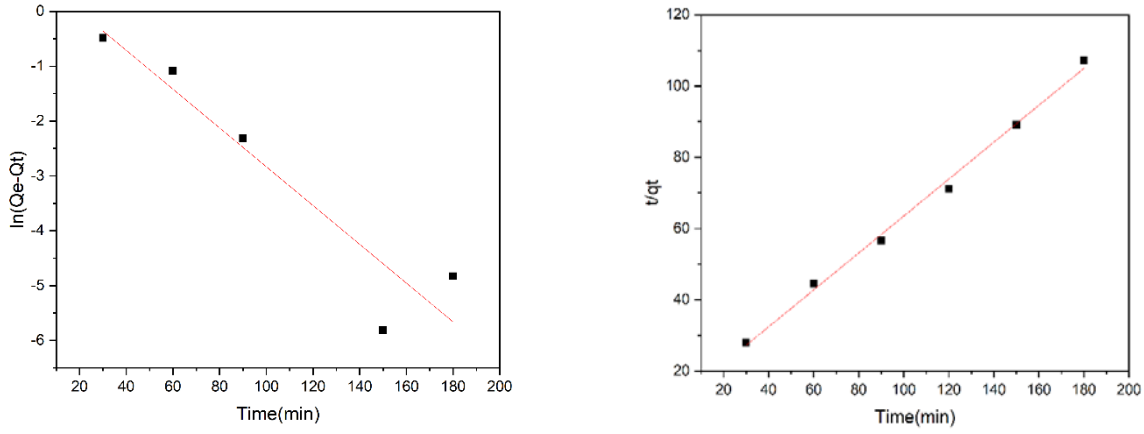

a) b)

Fig. 10. (a). Pseudo-first-order (b). pseudo-second-order kinetic plots for the Pb(II) adsorption onto ACCHM (adsorbent dose = 0.05 g, pH = 5±0.2 initial concentration = 2 mg/L, agitation speed = 60 rpm, T=303±2 K)

Further, the results revealed that the adsorption process might take place by chemisorption via the formation of coordinate bonds between electron rich binding sites of the adsorbent and adsorbate molecules.[31]

Kinetics parameters for pseudo-first order and pseudo-second-order models are tabulated in Table 3.

Table 3. Kinetic parameters for adsorption of Pb(II) onto ACCHM

Pseudo-first-order kinetic model		
K_1, (min^{-1})	q_e (mg/g)	R^2
0.0814	0.3517	0.8933
Pseudo-second-order kinetic model		
$K_{2,\,ads}$(g/ (mg min))	q_e (mg/g)	R^2
0.0229	1.9297	0.9955

4. Conclusions

In this study, AC and chitosan were prepared successfully using low-cost, readily available rice husks and shrimp shells, respectively. Upon coating of synthesized chitosan on the AC derived from rice husk, a novel AC/chitosan hybrid material (ACCHM) acquired surface properties of both AC and chitosan, including a highly functionalized porous surface, leading to enhanced metal adsorption capacity. Optimal adsorption performance (89% Pb removal) of the novel hybrid material was observed at pH = 5, initial Pb(II) concentration of 2 mg/L with a shaking time of 120 minutes of 1 g/L of ACCHM dosage. According to the isotherm studies, equilibrium data were fitted well with the Langmuir isotherm model (R^2 = 0.9916), indicating that Pb adsorption occurs on a

homogeneous adsorbent surface via monolayer adsorption. Further, the kinetics study showed that adsorption data were best fitted to pseudo-second-order kinetics ($R^2 = 0.9955$) indicating that Pb absorbed on the ACCHM surface by chemisorption. The findings of the study revealed that the novel hybrid material, ACCHM, can be used as an efficient, environmentally friendly, and cost-effective adsorbent for the removal of heavy metals such as Pb(II) from water.

Acknowledgements

Authors would like to acknowledge Amila T. Kannangara, S.A.A.K. Suriyaarachchi, and Erandi Udayasiri for supporting the analysis of samples.

References

[1] Bolan, N.S.; Adriano, D.C.; Naidu R. Role of Phosphorus in (Im)mobilization and Bioavailability of Heavy Metals in the Soil-Plant System. In *Reviews of Environmental Contamination and Toxicology*; Springer: New York, 2003; pp 1-44. https://doi.org/10.1007/0-387-21725-8_1

[2] Heil, D.M.; Samani, Z.; Hanson, A.T.; Rudd B. Remediation of Lead Contaminated Soil by EDTA. I. Batch and Column Studies. *Water Air Soil Pollut*. **1999**, *113*, 77–95. https://doi.org/10.1023/A:1005032504487

[3] Matlock, M.M.; Howerton, B.S.; Atwood, D.A. Irreversible Precipitation of Mercury and Lead. *J. Hazard. Mater.***2001**, *84*, 73–82. https://doi.org/10.1016/S0304-3894(01)00190-X

[4] Tao, Y.; Ye, L.; Pan, J.; Wang, Y.; Tang, B. Removal of Pb(II) from Aqueous Solution on Chitosan/TiO_2 Hybrid Film. *J. Hazard. Mater*. **2009**, *161*, 718–722. https://doi.org/10.1016/j.jhazmat.2008.04.012

[5] Fu, F.; Wang, Q. Removal of Heavy Metal Ions from Wastewaters: A Review. *J. Environ. Manage*. **2011**, *92*, 407–418. https://doi.org/10.1016/j.jenvman.2010.11.011

[6] Demirbas, A. Heavy Metal Adsorption onto Agro-Based Waste Materials: A Review. *J. Hazard. Mater*. **2008**, *157*, 220–229. https://doi.org/10.1016/j.jhazmat.2008.01.024

[7] Fiyadh, S.S.; AlSaadi, M.A.; Jaafar, W.Z.; AlOmar, M.K.; Fayaed, S.S.; Mohd, N.S.; Hin, L.S.; El-Shafie, A. Review on Heavy Metal Adsorption Processes by Carbon Nanotubes. *J. Clean. Prod*. **2019**, *230*, 783–793. https://doi.org/10.1016/j.jclepro.2019.05.154

[8] Dias, J.M.; Alvim-Ferraz, M.C.; Almeida, M.F.; Rivera-Utrilla, J.; Sánchez-Polo, M. Waste Materials for Activated Carbon Preparation and its Use in Aqueous-Phase Treatment: A Review. *J. Environ. Manage*. **2007**, *85*, 833–846. https://doi.org/10.1016/j.jenvman.2007.07.031

[9] Jusoh, A.; Shiung, L.S.; Noor, M.J.M.M. A Simulation Study of the Removal Efficiency of Granular Activated Carbon on Cadmium and Lead. *Desalination* **2007**, *206*, 9–16. https://doi.org/10.1016/j.desal.2006.04.048

[10] Jadhav, A.; Mohanraj, G. Synthesis of Activated Carbon from *Cocos nucifera* Leaves Agrowaste by Chemical Activation Method. *Chem. Chem. Technol*. **2016**, *10*, 201–208. https://doi.org/10.23939/chcht10.02.201

[11] Macalalad, A.; Ebete, Q.R.; Gutierrez, D.; Ramos, M.; Magoling, B.J. Kinetics and Isotherm Studies on Adsorption of Hexavalent Chromium Using Activated Carbon from Water Hyacinth. *Chem. Chem. Technol*. **2021**, *15*, 1–8. https://doi.org/10.23939/chcht15.01.001

[12] Abdulrazak, S.; Hussaini, K.; Sani, H.M. Evaluation of Removal Efficiency of Heavy Metals by Low-Cost Activated Carbon Prepared from African Palm Fruit. *Appl. Water Sci*. **2017**, *7*, 3151–3155. https://doi.org/10.1007/s13201-016-0460-x

[13] Hasanzadeh, M.; Simchi, A.; Shahriyari, F.H. Nanoporous Composites of Activated Carbon-Metal Organic Frameworks for Organic Dye Adsorption: Synthesis, Adsorption Mechanism and Kinetics Studies. *J. Ind. Eng. Chem*. **2020**, *81*, 405–414. https://doi.org/10.1016/j.jiec.2019.09.031

[14] Silva, T.L.; Cazetta, A.L.; Souza, P.S.C.; Zhang, T.; Asefa, T.; Almeida, V.C. Mesoporous Activated Carbon Fibers Synthesized from Denim Fabric Waste: Efficient Adsorbents for Removal of Textile Dye from Aqueous Solutions. *J. Clean. Prod*. **2018**, *171*, 482–490. https://doi.org/10.1016/j.jclepro.2017.10.034

[15] Patnukao, P.; Kongsuwan, A.; Pavasant, P. Batch Studies of Adsorption of Copper and Lead on Activated Carbon from *Eucalyptus camaldulensis Dehn*. Bark. *J. Environ. Sci*. **2008**, *20*, 1028–1034. https://doi.org/10.1016/S1001-0742(08)62145-2

[16] Guo, H.-L.; Wang, X.-F.; Qian, Q.-Y.; Wang, F.-B.; Xia, X.-H. A Green Approach to the Synthesis of Graphene Nanosheets. *ACS nano* **2009**, *3*, 2653–2659. https://doi.org/10.1021/nn900227d

[17] Guo, M; Qiu, G.; Song, W. Poultry Litter-Based Activated Carbon for Removing Heavy Metal Ions in Water. *Waste Manage*. **2010**, *30*, 308–315. https://doi.org/10.1016/j.wasman.2009.08.010

[18] Gerente, C.; Lee, V.K.C.; Le Cloirec, P.; McKay, G. Application of Chitosan for the Removal of Metals From Wastewaters by Adsorption – Mechanisms and Models Review. *Crit Rev Environ Sci Technol* **2007**, *37*, 41–127. https://doi.org/10.1080/10643380600729089

[19] Dutta, P.K.; Pradeep; Dutta, J.; Tripathi, V.S. Chitin and Chitosan: Chemistry, Properties and Applications. *J. Sci. Ind. Res*. **2004**, *63*, 20–31.

[20] Kalyani, S.; Krishnaiah, A.; Boddu, V.M. Adsorption of Divalent Cobalt from Aqueous Solution onto Chitosan–Coated Perlite Beads as Biosorbent. *Sep Sci Technol* **2007**, *42*, 2767–2786. https://doi.org/10.1080/01496390701511457

[21] Hydari, S.; Sharififard, H.; Nabavinia, M.; Parvizi, M.R. A Comparative Investigation on Removal Performances of Commercial Activated Carbon, Chitosan Biosorbent and Chitosan/Activated Carbon Composite for Cadmium. *Chem. Eng. J*. **2012**, *193-194*, 276–282. https://doi.org/10.1016/j.cej.2012.04.057

[22] Khan, T.A.; Peh, K.K.; Ch'ng, H.S. Reporting Degree of Deacetylation Values of Chitosan: The Influence of Analytical Methods. *J. Pharm. Pharmaceut. Sci*. **2002**, *5*, 205–212.

[23] Laine, J.; Calafat, A.; labady, M. Preparation and Characterization of Activated Carbons from Coconut Shell Impregnated with Phosphoric Acid. *Carbon* **1989**, *27*, 191–195. https://doi.org/10.1016/0008-6223(89)90123-1

[24] Paluszkiewicz, C.; Stodolak, E.; Hasik, M.; Blazewicz, M. FT-IR Study of Montmorillonite–Chitosan Nanocomposite Materials. *Spectrochim. Acta A Mol. Biomol. Spectrosc*. **2011**, *79*, 784–88. https://doi.org/10.1016/j.saa.2010.08.053

[25] Priyadarshini, B.; Rath, P. P.; Behera, S.S.; Panda, S.R.; Sahoo, T.R.; Parhi, P.K. Kinetics, Thermodynamics and Isotherm Studies on Adsorption of Eriochrome Black-T from Aqueous Solution Using Rutile TiO_2. *IOP Conf. Ser.: Mater. Sci. Eng*. **2018**, 012051. http://doi.org/10.1088/1757-899X/310/1/012051

[26] Nethaji, S.; Sivasamy, A.; Mandal, A.B. Adsorption Isotherms, Kinetics and Mechanism for the Adsorption of Cationic and Anionic Dyes onto Carbonaceous Particles Prepared from *Juglans regia* Shell Biomass. *Int J Environ Sci Technol (Tehran)* **2013**, *10*, 231–242. https://doi.org/10.1007/s13762-012-0112-0
[27] Sharma, M.; Hazra, S.; Basu, S. Kinetic and Isotherm Studies on Adsorption of Toxic Pollutants Using Porous ZnO@SiO_2 Monolith. *J. Colloid Interface Sci*. **2017**, *504*, 669–679. https://doi.org/10.1016/j.jcis.2017.06.020
[28] Achmad, A.; Kassim, J.; Suan, T.K.; Amat, R.C.; Seey, T.L. Equilibrium, Kinetic and Thermodynamic Studies on the Adsorption of Direct Dye onto a Novel Green Adsorbent Developed from Uncaria Gambir Extract. J. *Phys. Sci*. **2012**, *23*, 1–13.
[29] Cacicedo, M.L.; Manzo, R.M.; Municoy, S.; Bonazza, H.L.; Islan, G.A.; Desimone, M.; Bellimo, M.; Mammarella, E.J.; Castro, G.R. Immobilized Enzymes and their Applications. In *Advances in Enzyme Technology*; Singh, R.S.; Singhania, R.R., Eds.; Christian Larroche Elsevier, 2019; pp.169-200. https://doi.org/10.1016/B978-0-444-64114-4.00007-8
[30] Gao, W.; Majumder, M.; Alemany, L.B.; Narayanan, T.N.; Ibarra, M.A.; Pradhan, B.K.; Ajayan, P.M. Engineered Graphite Oxide Materials for Application in Water Purification. *ACS Appl. Mater. Interfaces* **2011**, *3*, 1821–1826. https://doi.org/10.1021/am200300u
[31] Yu, H.; Zha, B.; Chaoke, B.; Li, R.; Xing, R. High-efficient Synthesis of Graphene Oxide Based on Improved Hummers Method. *Sci. Rep*. **2016**, *6*, 36143 https://doi.org/10.1038/srep36143

Received: August 21, 2022 / Revised: October 19, 2022 / Accepted: February 08, 2023

ВИГОТОВЛЕННЯ ГІБРИДНОГО МАТЕРІАЛУ НА ОСНОВІ АКТИВОВАНОГО ВУГІЛЛЯ/ХІТОЗАНУ ДЛЯ АДСОРБЦІЙНОГО ВИЛУЧЕННЯ PB(II)

Анотація. *У цьому дослідженні синтезовано новий, економічно ефективний та екологічно чистий гібридний матеріал на основі активованого вугілля/хітозану через поєднання поверхневих властивостей активованого вугілля, отриманого з рисового лушпиння, та хітозану, вилученого з панцирів креветок "Чорний тигр", з метою отримання високофункціоналізованого пористого матеріалу з підвищеною адсорбційною здатністю до адсорбції Pb(II) для очищення води.*

Ключові слова: *активоване вугілля, адсорбційне вилучення, біомаса, хітозан, плюмбум, пористий матеріал.*